Journal of Mechanical Engineering Research and Developments
ISSN: 1024-1752
CODEN: JERDFO
Vol. 43, No. 4, pp. 207-222
Published Year 2020

Artificial Vision System for the Identification and Registration of Gaps Road from A Motorcycle

Andrés Betancourt, César Peña, & Gonzalo Moreno*

Mechanical and Mechatronic Department – University of Pamplona - Colombia

*Corresponding Author Email: gmoren@unipamplona.edu.co

ABSTRACT: This article presents the development of an artificial vision system for the identification and registration of gaps road. A system composed of economic elements and easy acquisition such as a mobile phone, a linear projection laser, among others that are mounted on a motorcycle, is proposed. The system allows detecting gaps based on the deformations of the line projected by the laser, using an algorithm of artificial vision. The registration of the gaps includes the use of global geolocation instruments, which allows the reconstruction of the road's maps indicating the gap's location. Experimental tests are presented for equipment calibration as well as for final system verification. The system results show great potential despite its low cost.

KEYWORDS: Gaps; artificial vision; driving assistance; mobile devices; motorcycle; GPS.

INTRODUCTION

In the development of humanity, roads have been indispensable from the moment in which transport has been required; Currently, in Colombia, the national road network is managed by the National Roads Institute (INVIAS), which is responsible for the construction, habilitation, paving and improvement of these. According to the institute, the system is composed of three sectors, a primary network consisting of national roads such as highways, viaducts, tunnels, and bridges. The secondary system consists of the ways that connect each municipality with the primary networks, these roads are in charge of each department as far as its territorial coverage is concerned. Finally, is the tertiary network comprising roads within every municipality.

In many places within Colombian territory, it is evidenced that part of the road infrastructure is in deplorable condition, which causes breakdowns in vehicles and often causes accidents. Most of this affected infrastructure corresponds to tertiary roads, which are overseen by the municipalities. Consequently, the continued access of vehicles to these areas means that the probability of having an accident is higher. Therefore, it becomes a necessity to acquire relevant information about the poor state of the roads and that such is regularly updated [1,2,3].

As mentioned above, the country does not have the best road network system, which means that drivers must pay more attention to the state of the roads, which is normal, but remember the location of each of the gaps with which he had eye contact and had to maneuver the vehicle is something ever more complex. For this purpose and many others, ADAS (Advanced Driver Assistance Systems) systems are more popular today, according to Moujahid et al. [4], these techniques have evolved to the point that machine learning methods have been developed to make them more robust. How the ADAS system has communication with the user is through cognitive signals, or alerts, visualizations, or vibration [5,6,7].

Driver assistance systems are composed of devices that perform the intermediation between the process and the user, so there are concepts such as HMI (Human Machine Interface) [8,9,10], which allow the user to be informed and have control of the machine or process. The device, in addition to behaving as an interface, offers that which information technology has currently brought to people who transport themselves in vehicles, the comfort of obtaining data about their location in real-time or the detail of a specific route, this makes the user maintain the course of his trajectory between a point of origin and one of destination if he so wishes. However, the user does not get feedback on the road condition, which would facilitate further movement to the selected destination. This is why the development of this project is relevant, which will allow drivers to carry out their work in a more efficient way, with more excellent safety and taking care of their vehicle, all this can be achieved with the integration of artificial intelligence and prevention systems.

The problem of the poor state of the roads originates due to several factors, among which are: the expansion of cities, which leads to the creation of new ways, the age of existing roads, the weather, lack of maintenance, among others. All these factors cause road users to be exposed to accidents, vehicle damage, vehicular congestion and decreased productivity (figure 1).

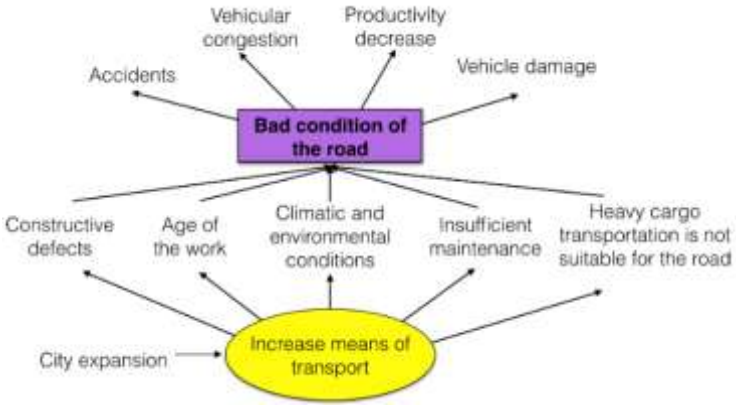

Figure 1. Problem Statement

Evidence of all these problems mentioned and their repercussions, this project seeks to solve the problem of the lack of easy-to-purchase and low-cost instruments that allow the detection of gaps in urban and inter-municipal roads. The objectives include the development of a system that will enable automatic registration of the location of the gaps using geo-location. Additionally, the system must use equipment that is easy to acquire. The system must be capable of mounting in a low-cost, fuel-efficient vehicle, such as motorcycles.

The article is organized as follows: Section 2 indicates the implementation of the artificial vision system and its description, in Section 3 the result obtained are detailed, and finally, the conclusions of the work done are given.

IMPLEMENTATION METHOD OF THE ARTIFICIAL VISION SYSTEM

The following stages determine project execution; in the first stage, there is a device that allows you to process images and/or videos, to examine the route or path taken by the vehicle. With the help of different programming algorithms based on artificial vision, aspects such as gaps, sinks, and sewers without cover were identified in the images. A similarity to this study is presented in the geodesic method [11], which deals with the study of land elevations, providing a representation of the shape and surface of a given space. This process is carried out through the implementation of an integrated laser system and a GPS.

The coordinates are obtained using GPS, a radio navigation system that provides reliable information about the location to users around the world, regardless of the atmospheric conditions in which the device is located [12,13,14]. For greater location accuracy, different electronic devices are used, together these allow access to global positioning information that pinpoints a location in latitude and longitude so that the acquired may be data mused in spreadsheets to subsequently make the proper registration in the Google Maps tool. This service allows the user to customize maps for their use or to share using the Application Programming Interfaces or APIs that the company has.

Mechatronic Design and Materials

The system is composed of different mechanical and electrical components, as shown in figure 2, that operate linked to each other to achieve the development of the proposed goal.

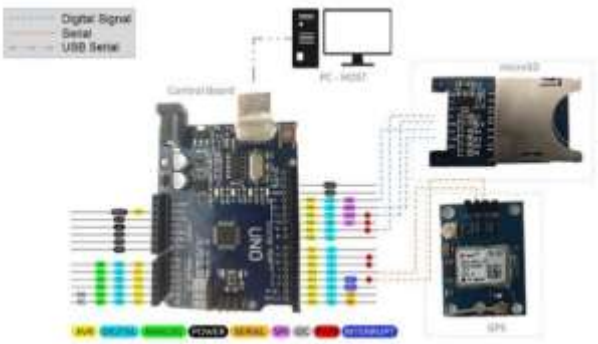

Figure 2. GPS Electronic Diagram

Image capture and recognition devices

A camera with the following characteristics was used to take the picture: 16 Megapixel camera resolution, 2.0 focal aperture, 27mm wide-angle lens, Omnivision OV13850, table (1) shows the laser device and its characteristics. This laser, when projected on a surface takes the form of a straight line thanks to the diffraction it suffers through a lens located in front of the system.

Table 1. Laser characteristics

Laser device	**Characteristics**	
	Power	200mW
	Operation Voltage	9v – 12v
	Spectrum	650nm
	Cable length	79cm
	Operating temperature	-20° - 70°
	Weight	45g
	Angle adjustment	90°

Electronic Devices

The GPS module Neo 6m (figure 2) has a ceramic antenna that facilitates the reception of the signal, which, thanks to its developed location system, can find an objective in a short time, even during challenging climatic conditions. The information provided by this module is processed through an algorithm implemented in an Arduino card from the programming interface, where instructions are given to carry out specific tasks.

Mechanical and Structural Elements

For the assembly of the cell phone in the vehicle (in this case, a motorcycle was used), a PLA structure and a cell phone holder were used, as can be seen in figure 3.

Figure 3. Cell phone holder - Motorcycle

Digital Image Treatment

In figure 4, the means of transport used for the project's implementation can be seen, the necessary devices for the execution and capture of how the laser behaves on the pavement before the treatment of the image obtained is contemplated.

Figure 4. Image Capture

For the system to identify the beam of light emitted by the laser and for the operation of the artificial vision system to begin its recognition processes, it is necessary to study several previously captured images (under different conditions such as lighting, type of floor or pavement, among others), for each of these images, the information is analyzed on a frequency basis using histograms in each layer of red (R), green (G) and blue (B) [13,15,16,17,18,19] corresponding to the section where the laser is projected. This information is intended to obtain the laser's range of color tones as well as the average in each of its components R, G, and B, which was 157, 48, and 50 correspondingly. With these values, we proceed to perform the artificial vision algorithm.

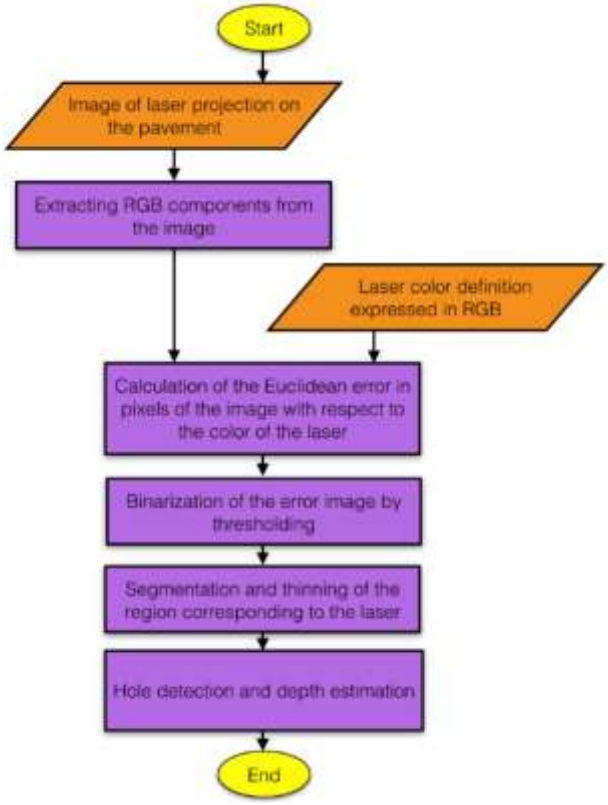

Figure 5. Image Processing Algorithm Flowchart.

The image processing algorithm flowchart is presented in figure 5. This algorithm aims to identify and segment only the laser line projected on the ground to detect whether there is a gap, as well as to estimate its depth.

First, an image of the path where the linear laser is projected is acquired. Subsequently, the image is broken down into three RGB components. All pixels of each of the layers are compared respecting the components of the target color (color defined for the laser) using Eq. (1) corresponding to the Euclidean error in the RGB color space.

Subsequently, it is determined if the line projected on the pavement continues to be straight or if otherwise, it changes in its natural form; if so, the system will confirm, and the data will be stored for analysis in the next stage of the algorithm.

$$E_{(i,j)} = \sqrt{\left(R_{(i,j)} - R_L\right)^2 + \left(G_{(i,j)} - G_L\right)^2 + \left(B_{(i,j)} - B_L\right)^2} \quad (1)$$

Where:

$E_{(i,j)}$: Pixel error in row *i* and column *j* of the image

$R_{(i,j)}, G_{(i,j)}, B_{(i,j)}$: Components in red (R), green (G), and blue (B) from the pixel in row *i* and column *j* of the image

R_L, G_L, B_L: Components in red (R), green (G), and blue (B) of the reference color corresponding to the laser.

In figure 6a, an example of a captured image is shown where the laser is projected on the pavement forming a straight line, and in figure 6b, the image representing the values corresponding to the Euclidean error respecting the target color (laser color). In this last image, it is highlighted that the lowest values (tend to black) correspond to those that coincide with the laser projection [11,16].

Figure 6. Laser's Image Projection on the Pavement **a)** original image **b)** image corresponding to the Euclidean error taking the laser's color as a reference

Next, a binarization of the image is carried out by thresholding values between zero and a predefined maximum that, in this case, is 30. (maximum allowed error); next, it takes the value of one, and the rest take the value of zero, as is seen in figure 6a. it can be evidenced that this binary image denotes the laser projection on the pavement.

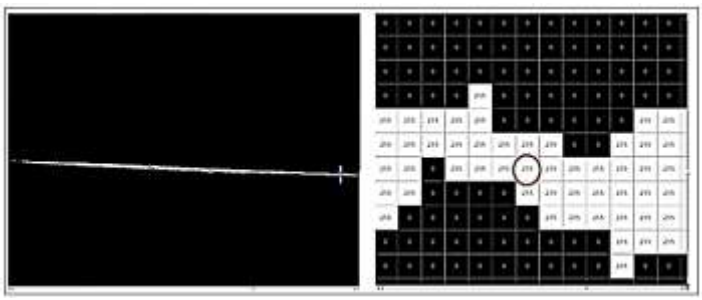

a) Binary image **b)** Binary image zoom

Figure 7. Binary Image

After obtaining the binary image (figure 7 (a)) the objective is to achieve slimming to form a one-pixel wide line. Then, the algorithm examines the image column by column and generates sets whose values correspond to the positions (in rows) of the pixels within the column, then the median of these sets is calculated, obtaining the central value in the position. An approach to the binary image is illustrated in figure 7 (b), and a circle indicates the central pixel of a particular column.

Once the entire procedure has been performed, the white line representing the laser projection on the track can be seen more clearly (see figure 8 (b)). The continuity of this line indicates that there are no gaps or potholes in the road. If there is a significant change (variations in positions on the vertical axis), the algorithm will assume that there is a gap and proceed to its estimation.

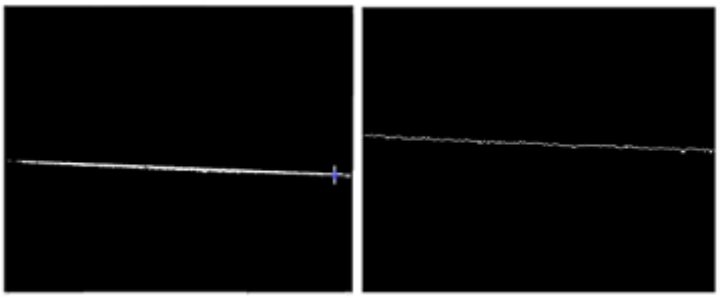

a) Binary image **b)** Slimming

Figure 8. Slimming Implementation

Figure 9 shows the application of the described algorithm in a situation where multiple factors affect the image's environment, such as water and mud. This figure shows how the vision algorithm does not enterely detect the laser

due to the significant variations in its colors. With the information obtained, the existence of the hole can be estimated; however, it cannot be correctly categorized.

Figure 9. Laser Identification Algorithm Test

To improve the robustness of the algorithm, the definition of the laser's color is extended by a set of tones that correspond to the laser's when it impacts different types of typical objects on the road. Figure 10 illustrates how the response to this type of situation improves dramatically (note that the green color represents the detection of the pixels corresponding to the laser).

Figure 10. Functional Algorithm Test for recognition

Gap Estimation Algorithm

To estimate the depth of the gaps, experimental tests were proposed in the laboratory where the devices are located on a structure or support of varying dimensions (see figure 11), and objects that interfere with the laser projection are located simulating the change in the height of the devices regarding the ground. The structure allows the fixing of the mobile device and the laser, allowing the graduation of its height and the projection angle of the laser and image.

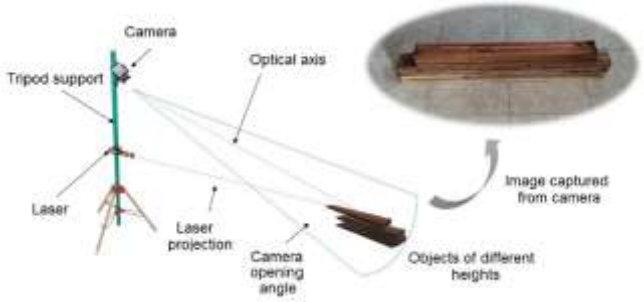

Figure 11. Tripod Support

For the digital treatment of the generated image, it is essential to know the location of the equipment and the references involved in the study, in figure 12 it can be seen that the reference system is located at the base of the structure from where you can detail the following distances: $\boldsymbol{h_L}$ is the height of the laser, $\boldsymbol{\alpha_L}$ is the rotation angle of the laser respecting the axis z, $\boldsymbol{h_C}$ is the height of camera location, $\boldsymbol{\alpha_C}$ is the camera rotation angle respecting the axis z, $\boldsymbol{h_s}$ is the vertical distance between the laser and the camera, the axis of the laser is defined by the segments $\boldsymbol{L_1}$ and $\boldsymbol{L_2}$, the optical axis of the camera is described by the two legs $\boldsymbol{C_1}$ and $\boldsymbol{C_2}$, $\boldsymbol{P_x}$ details the horizontal distance of the location of point P which represents the point of contact of the laser with the ground, segment A represents the distance that would be from the camera's axis to the point of incidence of the laser, this segment will be proportional to the number of pixels between the laser and the central row of the image taken by the camera.

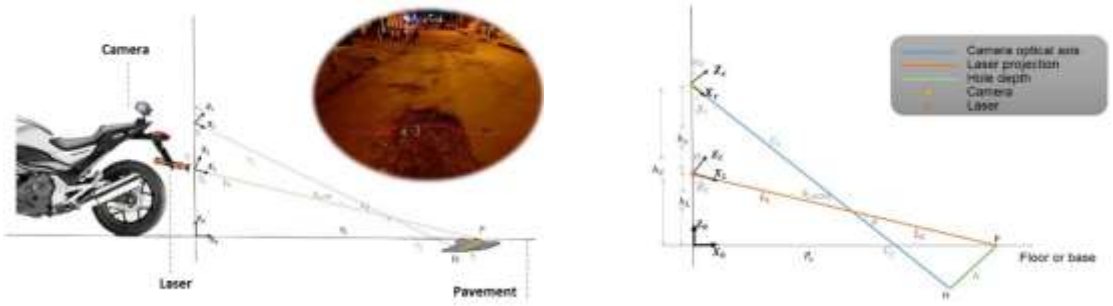

a) General Scheme **b)** Vector Diagram

Figure 12. System Scheme Camera-Laser Experiments

From figure 12, the following equations can be detailed:

$$\beta_c = 90 - \alpha_c \tag{2}$$

$$\beta_c + \alpha_L + 90 + \theta = 180 \tag{3}$$

Replacing (2) in (3) it is obtained:

$$\theta = \alpha_c - \alpha_L \tag{4}$$

The laser contact lines L_2 and L_2 are defined by:

$$L_2 = \frac{A}{\sin\theta} \tag{3}$$

$$L_1 = {}^{h_L}/_{\cos \beta_L} - L_2 \quad (4)$$

Additionally, the legs of the camera's optical axis can be detailed using Eqs. (7) and (8)

$$C_1 = \sqrt{h_s^2 + L_1^2 - 2h_s L_1 \cos(90 + \alpha_L)} \quad (7)$$

$$C_2 = L_2 \cos \theta \quad (8)$$

The following equation gives the horizontal distance (P_X) of the segment's location point that demarcates the gap:

$$P_x = (L_1 + L_2) \sin \beta_L \quad (9)$$

In system calibration, several tests were carried out to measure the height of the objects (see table (1)) that are on each other (as indicated in figure 11), tables (2) and (3) show the results of the studies carried out based on the geometric analysis of the system.

Table 2. Measurement – Experiment

# Objects	Height [cm]
1	2
2	4,8
3	7
4	9,5
5	11,5
6	13,5
7	16
8	18,4
9	20,5
10	22,5
11	24,3
12	26
13	28,8

In addition to the input data of the system (heights and orientation angles of the camera and the laser), in the table (3) and with the use of algorithms analysis, the distance A_P is calculated (distance in pixels from the optical axis of the camera to the incidence of the laser). A_m represents the magnitude of segment A, previously described in the geometric analysis of the mathematical model composed of the equations described in this section.

Table 3. Experiment Result Chart

Tests								
Sample	α_L [°]	α_C [°]	h_S [m]	h_C [m]	A_p	A_m	$A_{m-Regression}$	$h_{C2-Estimated}$
1	20	53	0,6	1,26	190	0,6899	0,6611	1,241
2	20	53	0,6	1,23	161	0,6421	0,6328	1,2241
3	20	53	0,6	1,21	137	0,6103	0,6094	1,2094
4	20	53	0,6	1,185	100	0,5705	0,5733	1,1868
5	20	53	0,6	1,165	79	0,5386	0,5528	1,1739
6	20	53	0,6	1,145	30	0,5068	0,505	1,1439
7	20	53	0,6	1,12	15	0,467	0,4903	1,1347
8	20	53	0,6	1,096	-27	0,4288	0,4493	1,2089
9	20	53	0,6	1,075	-13	0,3953	0,4045	1,0808
10	20	53	0,6	1,055	-105	0,3635	0,3732	1,0611
11	20	53	0,6	1,037	-152	0,3348	0,3273	1,0323
12	20	53	0,6	1,02	-191	0,3077	0,2893	1,0084
13	20	53	0,6	0,992	-231	0,2631	0,2502	0,9839

To get the results of the variable $A_{m-Regression}$ a linear regression was made from comparative data between A_m and A_P, to obtain a mathematical model that allows estimating the dimensions in meters of segment ***A*** from a distance given in pixels captured by the camera (see figure 13).

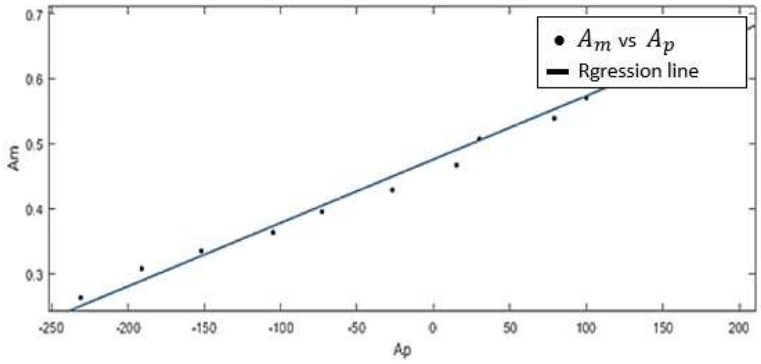

Figure 13. Regression Curve Ap vs Am

Subsequently, another algorithm is developed that calculates the height of the camera respecting the object impacted by the laser (gap) from the distance to the laser of the camera's optical axis in pixels. This allows recalculating the height of the camera ($h_{c2-Estimated}$), whereby, when compared to the actual height, the effectiveness of the image processing algorithm developed for this purpose can be predicted; this whole procedure allowed to select the best configuration for the measurement system.

GPS Positioning Algorithm

In determining the longitude and latitude coordinates, the assembly has a subsystem consisting of electronic devices connected, all leading to an instruction processing card based on the Arduino programming language. The Arduino IDE is a free software installed on the computer and allows the insertion of programming lines that are sequentially described in figure 14.

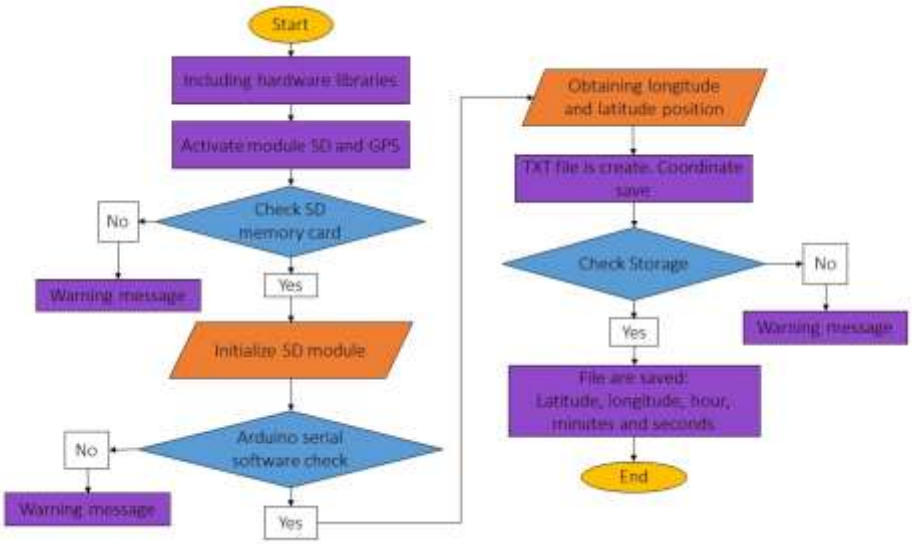

Figure 14. Arduino Algorithm Flowchart

The first block is composed of the inclusion of libraries required by the algorithm. The library “Timelib.h” facilitates the acquisition of a timer, used in this project to create a series of sequential time data that counts the process of coordinate capture, to specify in what second, minute or hour in that the hole has been detected. “TinyGPS.h” allows acquiring GPS data with specific commands, since the device grants them under the NMEA protocol regulation. “SD.h” is the library supporting instructions for writing or reading data from the SD card ready for storage.

The next block contains floating-type variables used in the algorithm, in which the longitude and latitude values are saved, followed by the creation of the objects, corresponding to the GPS, the file “sd_data” and the serial software. The conditional corresponds to the status of the SD module, if the initialization of the library is true the instructions follow the flow; otherwise, an error is sent that is sent on the serial port.

The algorithm cycle is determined by a conditional “while” that frequently evaluates the availability of the GPS device so that it is sending or receiving data. If the answer is positive, the reading of longitude and latitude stored in the pointers "& latitude" and "& longitude" is ordered. The creation of the text file is given by the instruction “SD.open” and saved under the name “data.txt”. Final verification of a conditional evaluates the behavior of the SD module, aiming to save information in it if the conditional claims to do so.

RESULTS AND DISCUSSION

In the field test, the system was installed on the back of a motorcycle (see figure 15) [17,20,21], which made a predetermined route in the urban area of the city of Fusagasuga - Colombia.

a) Image **b)** System

Figure 15. Testing and Implementation

Gap Identification

To indicate the laser's identification, an algorithm was developed that highlights the pixels that it recognizes as belonging to it using green. (See figure 16).

Figure 16. Laser Identification

A plot of the laser line's recognition is shown in figure 17, along with a straight dotted line of red, which represents the area where the laser should impact if there were no gaps. The laser deviation from the dotted line indicates the presence or not of gaps. In the case of figure 17, the existence of a gap can be quickly verified. In turn, by measuring this deviation through the algorithm presented in section 2.3, the depth of the gap can be estimated and characterized to indicate whether it is critical, acceptable, or light. When conducting the experimental tests, it was evidenced that the system successfully detected the gaps on the track. The estimated success rate is 95%.

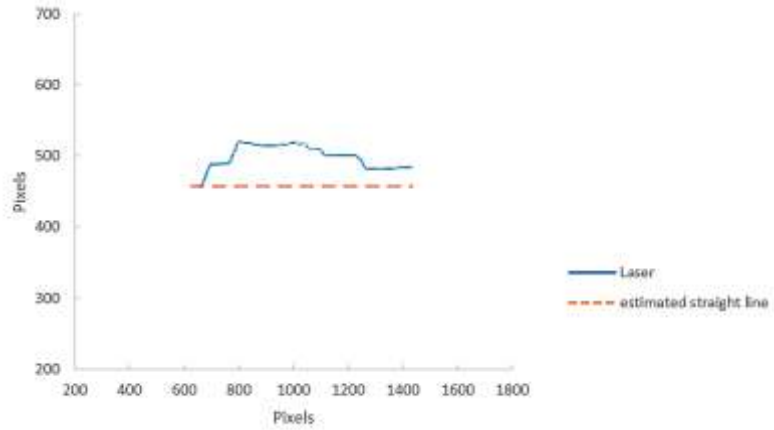

Figure 17. Laser Representation

Graphical User Interface (GUI) and Results

Figure 18. Database and Geolocation

Once the GPS connection is established, the results are visualized through a programming algorithm from the programming interface; instructions are given to carry out a specific task to obtain positioning.

The data supplied by the GPS is stored in the SD memory in a .txt file or a **csv** format, with two columns stored, one for longitude and one for latitude. If desired, a third column indicating the time in which the event was registered can be included.

Once the experiment is done, the file is loaded using a GPS coordinate display web software (GPS Visualizer - OpenStreetMap.org) to generate the geographic location of the collected points. Figure 18 illustrates the process performed, as well as an example of the representation of the geolocation of an experiment, where the red line represents the route taken by the vehicle.

This geolocation information can be exported to the Google application called My Maps, converting the captured data to a KML format; this is achieved on the same GPS Visualizer page. The application gives the option to share the map in social networks, email, and as a static map API, which allows the interactive created map to be included on a developer's website. Figure 19 shows the map obtained from an experiment and also indicates the place where holes were found.

Figure 19. Path and Gap Display

Graphical User Interface

For presentation and management by the user of the application, the system is represented in a friendly interface, which stands out for its simplicity and ease of operation. In figure 20, the boxes show different stages of execution of the artificial vision process. The upper left section shows the route made by the vehicle that owns the system; the route is traced and visualized thanks to the GPS Visualizer website and supported by Open Street Maps (OSM technology); followed by a video image on its left side. The transition of video frames captured by the camera. In the lower part, the results of the laser recognition algorithm are illustrated both in images and through labels that indicate the presence of gaps.

Figure 20. Graphical User Interface

Discussion

When evaluating the results obtained, it was evident that the developed device meets several desired characteristics such as: portability, its design implements elements of low cost and easy acquisition, it has a very intuitive user interface, the image processing algorithm is robust, efficient, effective, in addition to being simple to implement, requiring low computing power.

The experimental results showed that the device has excellent precision and is capable of estimating gaps with an average error of 7mm, without taking out layer into account. This precision is ideal for the task, considering that it is desired to detect holes of medium (25 to 50mm) and large (bigger than 50mm) sizes [2]. The geolocation of the holes is recorded with an error of less than ± 3m, which is good for generating the reports.

CONCLUSIONS

The system has been developed by adding different low-cost electronic components that are synchronized and put into operation with the ordering of computer instructions to achieve the identification of holes in the asphalt.

The programming algorithm of the embedded system proved to be effective and required a little computational cost, which implies cost reduction and reduced execution times. Similarly, the signal processing algorithm is high-speed and detects gaps with high precision. Experimental tests showed that through this sensor, the gaps could be properly characterized.

Experimental tests showed some adversities, which imply some limitations in the use of the system. Some of them are used at times where the sun is not at its maximum splendor since the intense light can affect the accuracy of the system. For this case, it is recommended to cover the laser projection on the pavement or, failing that, perform the scans before 10 am or after 4 pm depending on the weather conditions. On the other hand, it is also recommended to avoid using the system during or after the rain, since water can reflect the laser, generating inaccuracies in the estimation of the gaps.

The GPS module works with high precision; the different weather conditions are not a problem to it. It is possible to obtain the georeference points emitted by the module and made available in a microSD. The graphical interface developed evidence to be very intuitive and, therefore, easy to handle.

REFERENCES

[1] I. Silva, “Reconstrucción tridimensional de objetos mediante técnicas evolutivas”. [Diss. Tesis Doctoral]. *Centro de Investigación y de Estudios Avanzados del Instituto Politécnico Nacional*, México DF, 2008.

[2] F. A. Gutiérrez, "Estudio e investigación del estado actual de las obras de la red nacional de carreteras." *Manual para la inspección visual de pavimentos flexibles. Ministerio de Transporte, Republica de Colombia.* Bogotá DC, 2006.

[3] A. R. Morantes, G. G. Contreras and B. A. Valencia, “Risk Analysis of Heavy Vehicles Accidents on the Cúcuta – Pamplona Road”. *Revista Colombiana de Tecnologías de Avanzada* (RCTA), Vol 3. No. 32, Pp 74-79, 2019.

[4] A. Moujahid, M. E. Tantaoui, M. D. Hina, A. Soukane, A., Ortalda, A., ElKhadimi, and A. Ramdane-Cherif, "Machine learning techniques in ADAS: a review." *2018 International Conference on Advances in Computing and Communication Engineering (ICACCE)*. IEEE, 2018. doi: 10.1109/ICACCE.2018.8441758

[5] S. M. Sarala, D. H. Sharath Yadav and A. Ansari. "Emotionally Adaptive Driver Voice Alert System for Advanced Driver Assistance System (ADAS) Applications." *2018 International Conference on Smart Systems and Inventive Technology (ICSSIT)*. IEEE, 2018. doi: 10.1109/ICSSIT.2018.8748541

[6] L. Meng, K. Wevers, and R. V. Heijden. "Technical feasibility of advanced driver assistance systems (ADAS) for road traffic safety." *Transportation Planning and Technology* 28.3: 167-187, 2005.

[7] C. Kedar, R. Staszewski, and G. Agarwal. "TI vision SDK, optimized vision libraries for ADAS systems." *White Paper: SPRY260, Texas Instrument Inc*. 2014.

[8] B. Paul, R. Paul, and S. W. Kercel. "Sensory substitution and the human–machine interface." *Trends in cognitive sciences* Vol. 7, No. 12. Pp 541-546. 2003.

[9] P., Deborah L., Eliana MO Peres, and R. A. Evans. "Human machine interface for telephone feature invocation." *U.S. Patent No. 5,533,110*. 2 Jul. 1996.

[10] J.J. Charles, T. C. Wingrove, and R. D. Channey. "Finger pointing, gesture based human-machine interface for vehicles." *U.S. Patent No. 8,760,432*. 24 Jun. 2014.

[11] J. Hernández, P. Paredes, D. Carrion and A. Rivera, "Ice elevation changes surveyed with Airborne laser scanning data." *2017 First IEEE International Symposium of Geoscience and Remote Sensing (GRSS-CHILE)*. IEEE, 2017. doi: 10.1109/GRSS-CHILE.2017.7996012

[12] M. Zelang and S. Wenzhong, "Road centreline extraction from classified images by using the geodesic method." *Remote sensing letters*, Vol 5, No. 4, Pp 367-376. 2014.

[13] A.Dedi, N.H. Ausi, and C. A. Rohkmana. "Developing Android Application for Precise Geotagging using RTK GPS Module." *2018 4th International Conference on Science and Technology (ICST)*. IEEE, 2018. DOI: 10.1109/ICSTC.2018.8528570

[14] I Alexander. "Perspective/navigation-the global positioning system." *IEEE spectrum, Vol.* 30, No.12, Pp 36-38. 1993. DOI: 10.1109/6.272176

[15] Qingbo, Zhu. "Pavement crack detection algorithm Based on image processing analysis." *2016 8th International Conference on Intelligent Human-Machine Systems and Cybernetics (IHMSC)*. Vol. 1. IEEE, 2016. DOI: 10.1109/IHMSC.2016.96

[16] Muñoz, A. V. "Principios de color y holopintura". *Editorial Club Universitario.* ISBN: 8415787081. 2013.

[17] K., G. Arun, A Santhosh, A Ajith and T Maharajothi "Road quality management system using mobile sensors." *2017 International Conference on Innovations in Information, Embedded and Communication Systems (ICIIECS)*. IEEE, 2017. DOI: 10.1109/ICIIECS.2017.8276014

[18] L. Xin, and Y. Shi. "Computer vision imaging based on artificial intelligence." *2018 International Conference on Virtual Reality and Intelligent Systems (ICVRIS)*. IEEE, 2018. DOI: 10.1109/ICVRIS.2018.00014

[19] H. P. Lin, P. H. Liao,and Y. L. Chang, "Long-Distance Vehicle Detection Algorithm at Night for Driving Assistance." *In 2018 3rd IEEE International Conference on Intelligent Transportation Engineering (ICITE)* Pp. 296-300, 2018. doi: 10.1109/ICITE.2018.849262820

[20] D. Song, H. N. Lee, J. Yi and A. Levandowski, "Vision-based motion planning for an autonomous motorcycle on ill-structured roads." *Autonomous Robots*, 23(3), pp197-212, 2007.

[21] S. Messelodi, C. M. Modena and G. Cattoni, "Vision-based bicycle/motorcycle classification." *Pattern recognition letters*, Vol. 28, No. 13, Pp 1719-1726, 2007.